Inorg. Chem. **2008**, *47*, 8921−8931

The Key Role of the Intermolecular $\pi-\pi$ Interactions in the Presence of Spin Crossover in Neutral [Fe(abpt)$_2$A$_2$] Complexes (A = Terminal Monoanion N Ligand)

Gaelle Dupouy,[†] Mathieu Marchivie,[†] Smail Triki,*[,†] Jean Sala-Pala,[†] Jean-Yves Salaün,[†] Carlos J. Gómez-García,[‡] and Philippe Guionneau[§]

UMR CNRS 6521, Université de Bretagne Occidentale, BP 809, 29285 Brest Cedex, France, Instituto de Ciencia Molecular, Universidad de Valencia, 46980 Paterna, Valencia, Spain, and ICMCB, UPR CNRS 9048, Av. du docteur Schweitzer, 33608 Pessac, France

Received May 27, 2008

New iron(II) complexes of formulas [Fe(abpt)$_2$(tcm)$_2$] (**1**), [Fe(abpt)$_2$(tcnome)$_2$] (**2**), and [Fe(abpt)$_2$(tcnoet)$_2$] (**3**) (abpt = 4-amino-3,5-bis(pyridin-2-yl)-1,2,4-triazole, tcm$^-$ = [C(CN)$_3$]$^-$ = tricyanomethanide anion; tcnome$^-$ = [(NC)$_2$CC(OCH$_3$)C(CN)$_2$]$^-$ = 1,1,3,3-tetracyano-2-methoxypropenide anion; tcnoet$^-$ = [(NC)$_2$CC(OC$_2$H$_5$)C(CN)$_2$]$^-$ = 1,1,3,3-tetracyano-2-ethoxypropenide anion) have been synthesized and characterized by infrared spectroscopy, magnetic properties and by variable-temperature single-crystal X-ray diffraction. The crystal structure determinations of **1** and **2** reveal in both cases centrosymmetric discrete iron(II) monomeric structures in which two abpt chelating ligands stand in the equatorial plane and two terminal polynitrile ligands complete the distorted octahedral environment in trans positions. For **3**, the crystallographic studies revealed two polymorphs, **3-A** and **3-B**, exhibiting similar discrete molecular structures to those found for **1** and **2** but with different molecular arrangements. In agreement with the variable-temperature single-crystal X-ray diffraction, the magnetic susceptibility measurements, performed in the temperature range 2−400 K, showed a spin-crossover phenomenon above room temperature for complexes **1**, **3-A**, and **3-B** with a $T_{1/2}$ of 336, 377, and 383 K, respectively, while complex **2** remains in the high-spin ground state ($S = 2$) in the whole temperature range. To understand further the magnetic behaviors of **1**, **3-A**, and **3-B**, single-crystal X-ray diffraction measurements were performed at high temperatures. The crystal structures of both polymorphs could not be obtained above 400 K because the crystals decomposed. However, single-crystal X-ray data have been collected for compound **1**, which reaches the full high-spin state at lower temperatures. Its crystal structure, solved at 400 K, showed a strong modification of the iron coordination sphere (average Fe−N = 2.157(3) Å vs 1.986(3) Å at 293 K). In agreement with the magnetic properties. Such structural behavior is a signature of the spin-state transition from low-spin (LS) to high-spin (HS). On the basis of the intermolecular π stacking observed for the series described in this paper and for related complexes involving similar discrete structures, we have shown that complexes displaying frontal π stacking present spin transition such as **1**, **3-A**, and **3-B** and those involving sideways π stacking such as complex **2** remain in the HS state.

Introduction

Spin-transition complexes have been widely investigated for the past 30 years.[1−6] The spin-crossover (SCO) phenomenon particularly interests the scientific community, according to the large number of interesting behaviors observed and the possibility to record information reversely, without any fatigability. Iron(II) metal complexes involving the octahedral coordination sphere [FeN$_6$] are the most

* Author to whom correspondence should be addressed. E-mail: triki@univ-brest.fr.
[†] Université de Bretagne Occidentale.
[‡] Universidad de Valencia.
[§] UPR CNRS 9048.

(1) Toftlund, H. *Coord. Chem. Rev.* **1989**, *94*, 67.
(2) König, E. *Struct. Bonding (Berlin)* **1991**, *76*, 51.
(3) König, E.; Ritter, G.; Kulshreshtha, S. K. *Chem. Rev.* **1985**, *85*, 219.
(4) Gütlich, P.; Hauser, A. *Coord. Chem. Rev.* **1990**, *97*, 1.
(5) Gütlich, P. *Struct. Bonding (Berlin)* **1981**, *44*, 83.
(6) Gütlich, P.; Garcia, Y.; Spiering, H. *Magnetism: molecules to materials IV*; Miller, J. S., Ed.; Wiley-CH: New York, 2003.

10.1021/ic800955r CCC: $40.75
Published on Web 08/08/2008

Scheme 1

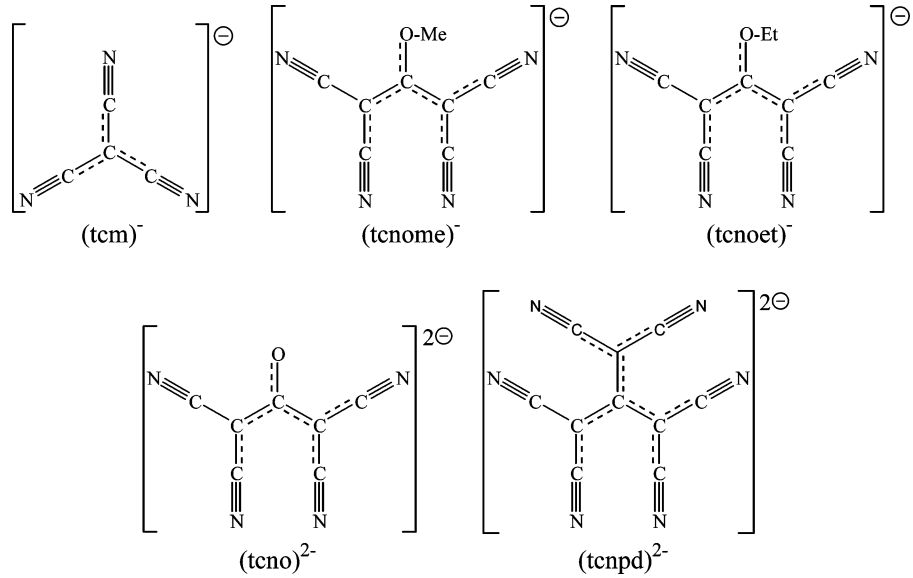

studied SCO compounds. When the ligand field energy approaches the thermal energy, a SCO transition between the high-spin state (HS; $S = 2$, $^5T_{2g}$) and low-spin state (LS; $S = 0$, $^1A_{1g}$) can be induced by different external stimuli such as temperature, pressure, and light irradiation. As recently noted,[7] most of these $[FeN_6]$ SCO compounds can be roughly divided into two categories: The first category is one in which the six donating-nitrogen atoms arise from neutral ligands to generate the $[FeL_x]^{2+}$ cationic complexes (L = tridentate ($x = 2$), bidentate ($x = 3$), monodentate ($x = 6$)), the anionic entities acting as simple noncoordinating counteranions. The second category corresponds to complexes in which four nitrogen atoms arise from neutral ligands, two monodentate anionic N ligands completing the octahedral environment of the iron ion, leading to the $[FeL_y(X)_2]$ neutral complexes, where X is a simple anionic ligand such as NCS^- and $NCSe^-$ and L is a tetradentate ($y = 1$), a bidentate ($y = 2$), or monodentate ($y = 4$) nitrogen-donating ligand.

One of the most interesting challenges nowadays is to control the SCO characteristics such as the temperatures and the abruptness of the transitions. Among the solutions which can be proposed to tune the transition temperatures, modifications of the anionic ligand linked to the metal ion in SCO systems of the second category appear very attractive. Previous studies have shown the effect of such a substitution in iron(II) complexes.[8−13] It is worth noting, however, that these studies concern a very limited number of anions and deal essentially with NCS^-, $NCSe^-$, $tcnq^{\bullet-}$ (tetracyanoquinodimethane radical anion), and dca^- (dicyanamide anion).[7−15] Thus, the use of new families of anionic ligands for which the structural and electronic characteristics can be tuned by slight chemical or electrochemical modifications such as the substitution of functional groups or variation of the negative charge is a particularly attractive way to better understand their effects on the magnetic properties. In this context, we have reported, over the past few years, several series of magnetic coordination polymers based on various polynitrile anions (Scheme 1). From such studies, it was clearly established that these anions are interesting ligands because of their high electronic delocalization and their cyano groups juxtaposed in such a way that they cannot all coordinate to the same metal ion.[16−27] They adopt different bridging or nonbridging coordination modes which afford discrete or extended fascinating molecular architectures.

(7) Moliner, N.; Gaspar, A. B.; Muñoz, M. C.; Niel, V.; Cano, J.; Real, J.-A. *Inorg. Chem.* **2001**, *40*, 3991.
(8) Moliner, N.; Muñoz, M. C.; Létard, S.; Létard, J.-F.; Solans, X.; Burriel, R.; Castro, M.; Kahn, O.; Real, J.-A. *Inorg. Chim. Acta* **1999**, *291*, 279.
(9) Capes, L.; Létard, J.-F.; Kahn, O. *Chem.—Eur. J.* **2000**, *6*, 2246.
(10) Gaspar, A. B.; Carmen Munoz, M.; Moliner, N.; Ksenofontov, V.; Levchenko, G.; Guetlich, P.; Antonio Real, J. *Monatsh. Chem.* **2003**, *134*, 285.
(11) König, E.; Madeja, K. *Inorg. Chem.* **1967**, *6*, 48.
(12) Ksenofontov, V.; Gaspar, A. B.; Real, J.-A.; Gütlich, P. *J. Phys. Chem. B* **2001**, *105*, 12266.
(13) Little, B. F.; Long, G. J. *Inorg. Chem.* **1978**, *17*, 3401.
(14) Kunkeler, P. J.; Koningsbruggen, P. J. v.; Cornelissen, J. P.; Van der Horst, A. N.; Van der Kraan, A. M.; Spek, A. L.; Haasnoot, J. G.; Reedijk, J. *J. Am. Chem. Soc.* **1996**, *118*, 2190.
(15) Pillet, S.; Lecomte, C.; Sheu, C. F.; Lin, Y. C.; Hsu, I. J.; Wang, Y. *J. Phys.: Conf. Ser.* **2005**, *21*, 221.
(16) Atmani, C.; Setifi, F.; Benmansour, S.; Triki, S.; Marchivie, M.; Salaün, J.-Y.; Gómez-García, C. J. *Inorg. Chem. Commun.* **2008**, *11*, 921.
(17) Benmansour, S.; Setifi, F.; Triki, S.; Salaün, J.-Y.; Vandevelde, F.; Sala-Pala, J.; Gómez-García, C. J.; Roisnel, T. *Eur. J. Inorg. Chem.* **2007**, 186.
(18) Triki, S.; Thétiot, F.; Vandevelde, F.; Sala-Pala, J.; Gómez-García, C. J. *Inorg. Chem.* **2005**, *44*, 4086.
(19) Thétiot, F.; Triki, S.; Sala-Pala, J.; Galan-Mascaros, J.-R.; Martinez-Agudo, J. M.; Dunbar, K. R. *Eur. J. Inorg. Chem.* **2004**, 3783.
(20) Galan-Mascaros, J.-R.; Thétiot, F.; Triki, S.; Sala-Pala, J.; Dunbar, K. R. *J. Phys. IV* **2004**, *114*, 625.
(21) Thétiot, F.; Triki, S.; Sala-Pala, J.; Golhen, S. *Inorg. Chim. Acta* **2003**, *350*, 314.
(22) Thétiot, F.; Triki, S.; Sala-Pala, J. *Polyhedron* **2003**, *22*, 1837.
(23) Thétiot, F.; Triki, S.; Sala-Pala, J.; Gómez-García, C. J. *Dalton Trans.* **2002**, 1687.
(24) Triki, S.; Thétiot, F.; Galan-Mascaros, J.-R.; Sala-Pala, J.; Dunbar, K. R. *New J. Chem.* **2001**, *25*, 954.
(25) Triki, S.; Thétiot, F.; Sala-Pala, J.; Golhen, S.; ClementeJuan, J. M.; Gómez-García, C. J.; Coronado, E. *Chem. Commun.* **2001**, 2172.
(26) Triki, S.; Sala-Pala, J.; Decoster, M.; Molinié, P.; Toupet, L. *Angew. Chem., Int. Ed.* **1999**, *38*, 113.
(27) Triki, S.; Sala-Pala, J.; Riou, A.; Molinié, P. *Synth. Met.* **1999**, *102*, 1472.

Taking into account the crucial role of these anionic ligands, we are interested in using them in combination with other chelating or bridging neutral coligands to explore their structural and electronic characteristics in the large field of molecular materials exhibiting the SCO phenomenon, which is governed essentially by subtle changes in the structural packing and, therefore, by the nature of the polynitrile ligand.

We report here the syntheses, variable-temperature structural characterizations, and magnetic properties of the first series of SCO complexes involving polynitrile anions and the neutral coligand 4-amino-3,5-bis(pyridin-2-yl)-1,2,4-triazole (abpt): $[Fe(abpt)_2(tcm)_2]$ (**1**), $[Fe(abpt)_2(tcnome)_2]$ (**2**), and $[Fe(abpt)_2(tcnoet)_2]$ (**3**) ($tcm^- = [C(CN)_3]^- =$ tricyanomethanide anion; $tcnome^- = [(NC)_2CC(OCH_3)C(CN)_2]^- =$ 1,1,3,3-tetracyano-2-methoxypropenide anion; $tcnoet^- = [(NC)_2CC(OC_2H_5)C(CN)_2]^- =$ 1,1,3,3-tetracyano-2-ethoxypropenide anion). Compound **3** revealed the occurrence of two polymorphs (**3-A** and **3-B**), offering the possibility to underline the effect of a slight structural modification on the magnetic properties.

Experimental Section

Materials. Tetracyanoethylene, urea, potassium *tert*-butoxide (C_4H_9OK), malononitrile ($CH_2(CN)_2$), 4-amino-3,5-bis(pyridin-2-yl)-1,2,4-triazole (abpt), and iron(II) chloride tetrahydrate were purchased from commercial sources and used without further purification.

Syntheses of K(tcm) and K(tcnoet). The potassium tricyanomethanide (K(tcm)) and the potassium 1,1,3,3-tetracyano-2-ethoxypropenide (K(tcnoet)) were prepared following the previously described procedures.[22,28] **K(tcm).** Anal. calcd for KC_4N_3: C, 37.2; N, 32.5%. Found: C, 36.5; N, 31,5%. IR data (ν, cm^{-1}): 3419(br), 2831(w), 2177(s), 2128(m), 1653(w), 1635(w), 1457(w), 1273(w), 1253(w), 1239(w), 568(s). **K(tcnoet).** Anal. calcd for $KC_9H_5N_4O$: C, 48.2; N, 25.0; H, 2.3%. Found: C, 48.0; N, 24.9; H, 2.2. IR data (ν, cm^{-1}): 3427(br), 2999(w), 2986(w), 2204(s), 2166(m), 2149(m), 1653(w), 1635(w), 1497(s), 1425(s), 1379(m), 1348(m), 1187(m), 999(m). ^{13}C NMR ($CD_3(CO)CD_3$), δ: 15.4 (CH_3), 46.6 ($\underline{C}(CN)_2$), 71.2 (CH_2), 117.5 (CN), 182.5 ($\underline{C}$(OEt)).

Syntheses of K(tcnome) and (Et_4N)(tcnome). Potassium 1,1,3,3-tetracyano-2-methoxypropenide (K(tcnome)) was prepared in two steps using the following procedure: A solution of tetracyanoethylene (3.2 g, 25 mmol) and urea (0.5 g, 8 mmol) in methanol (15 mL) was warmed up to 35 °C and stirred for 30 min. The resulting yellow solution was mixed with freshly distilled diethyl ether and cooled to −80 °C. After 24 h, the suspension was filtered, and the resulting solid was extracted with freshly distilled diethyl ether at room temperature. The mixture was filtered again, and the resulting yellow solution was cooled down to −80 °C. After 1 day, a white crystalline powder of the acetal 1,1-dicyano-2,2-methoxyethylene ($C_6H_6N_2O_2$) was obtained by filtration at −80 °C (yield: 1.55 g, 45%). IR data (ν, cm^{-1}): 3446(br), 2962(w), 2226(s), 2209(s), 1559(s), 1487(s), 1419(m), 1351(s), 1239(m), 1220(m), 1138(m), 1004(m), 942(m), 716(m), 677(m). ^{13}C NMR (CD_3CN), δ: 43.63, 60.74, 114.63, 177.97.

In a second step, to a solution of malononitrile (0.478 g, 7.24 mmol) and potassium *tert*-butoxide (0.784 g, 7.24 mmol) in methanol (10 mL) was added a methanolic solution (15 mL) of the previously prepared acetal ($C_6H_6N_2O_2$, 1.00 g, 7.24 mmol). The resulting solution was refluxed for 2 h. After cooling to room temperature, the methanol was removed under vacuum, and the resulting solid was washed with freshly distilled diethyl ether and dried under vacuum. A pale yellow polycrystalline powder of potassium 1,1,3,3-tetracyano-2-methoxypropenide (Ktcnome) was obtained (yield: 1.07 g, 70%). Anal. calcd for $KC_8H_3N_4O$: C, 45.7; N, 26.6; H, 1.4%. Found: C, 46.0; N, 26.2; H, 1.5%. IR data (ν, cm^{-1}): 3447(br), 3349(br), 2208(s), 2176(s), 1663(s), 1647(s), 1558(m), 1486(s), 1465(m), 1439(sh), 1357(s), 1335(s), 1251(w), 1213(m), 1135(m), 954(m), 887(w), 802(w), 754(m), 710(m), 568(m), 547(m), 502(m), 547(m), 502(w), 475(m). ^{13}C NMR (CD_3CN), δ: 45.93 ($\underline{C}(CN)_2$), 62.27 (OCH_3), 117.33 ($\underline{C}N$), 182.46 ($\underline{C}$(OMe)).

The tetraethylammonium salt was prepared in two steps. To a concentrated aqueous solution of K(tcnome) (0.437 g, 2.08 mmol) was added under continuous stirring an aqueous solution of $AgNO_3$ (0.460 g, 2.71 mmol). The brown precipitate of Ag(tcnome) that formed immediately was filtered on a sintered, fritted glass and air-dried (0.555 g, 1.99 mmol). In the second step, an acetonitrile solution (30 mL) of tetraethylammonium chloride (0.315 g, 1.90 mmol) was added to the dried powder of Ag(tcnome) under continuous stirring, giving rise to an instantaneous white precipitate of AgCl, which was filtered out. Slow concentration of the brown filtrate at room temperature gave colorless needle crystals of (Et_4N)(tcnome), which were filtered and air-dried (yield: 0.540 g, 86%). Anal. calcd for $C_{16}H_{23}N_5O$: C, 63.8; N, 23.2; H, 7.7%. Found: C, 63.2; N, 23.6; H, 7.8%. IR data (ν, cm^{-1}): 3412(br), 3007(br), 2987(s), 2943(br), 2194(s), 2180(s), 1635(w), 1481(s), 1436(s), 1389(s), 1367(s), 1355(s), 1229(w), 1188(w), 1172(s), 1070(w), 1054(m), 998(s), 895(w), 786(s), 698(w), 567(w), 540(w), 469(w), 420(w).

Syntheses of $[Fe(abpt)_2(tcm)_2]$ (1) and $[Fe(abpt)_2(tcnome)_2]$ (2). Both complexes were prepared using similar procedures: To a water/methanol (1:1) solution (10 mL) of $FeCl_2 \cdot 4H_2O$ (50 mg, 0.25 mmol) was slowly added a solution of abpt (120 mg, 0.5 mmol) in methanol (20 mL). To the resulting red solution was added a solution of the polynitrile potassium salt (0.5 mmol of K(tcm) for **1**; 0.5 mmol of K(tcnome) for **2**) in water (20 mL). The mixture was then filtered, and the resulting solution was allowed to evaporate for a few days at room temperature. Red prismatic crystals of **1** and yellow prismatic crystals of **2** were obtained and air-dried (yield: 0.128 g, 72% for **1**; 0.149 g, 68% for **2**). **Complex 1.** Anal. calcd. for $FeC_{32}H_{20}N_{18}$: C, 54.0; N, 35.4; H, 2.8%. Found: C, 54.3; N, 35.0; H, 2.8%. IR data (ν, cm^{-1}): 3478(br), 3422(br), 3250(s), 2241(s), 2188(s), 2171(s), 1635(s), 1612(m), 1591(s), 1568(m) 1543(m), 1461(s), 1428(s), 1399(m), 1293(m), 1251(s), 1180(m), 1151(m), 1038(s), 912(m), 792(s), 746(s), 695(s), 640(m), 615(m), 552(m), 457(m), 407(m). **Complex 2.** Anal. calcd for $FeC_{40}H_{26}N_{20}O_2$: C, 55.0; N, 32.0; H, 3.0%. Found: C, 55.4; N, 31.8; H, 2.9%. IR data (ν, cm^{-1}): 3421(br), 3258(s), 2218(s), 2201(s), 2192(s), 1621(m), 1602(m), 1592(m), 1569(m) 1495(s), 1461(s), 1428(sh), 1395(sh), 1375(s), 1296(m), 1253(m), 1235(m), 1209(m), 1145(m), 1050(m), 1041(m), 1015(m), 966(m), 804(m), 790(s), 743(m), 700(s), 543(m), 426(m).

Synthesis of $[Fe(abpt)_2(tcnoet)_2]$ (3). This complex was obtained as prismatic red crystals using the procedure described above for complexes **1** and **2** (yield: 0.187 g, 83%). However, preliminary single-crystal studies showed that this compound crystallizes into two polymorphs (**3-A** and **3-B**). In order to settle specific experimental procedures to obtain each polymorph, we have performed several syntheses of **3** using a diffusion in silicate gel technique: 1 mL of tetramethoxysilane was added, under vigorous stirring, to an aqueous solution (10 mL) containing iron(II) chloride

(28) Carboni, R. A. *Org. Synth.* **1959**, *39*, 64.

tetrahydrate (0.050 g, 0.25 mmol) and K(tcnoet) (0.112 g, 0.5 mmol). The gel was formed after standing after 1 day at room temperature. An ethanolic solution (10 mL) containing abpt (0.015 mg, 0.063 mmol) was carefully added onto the gel. Single crystals of pure **3-B** were grown inside the gel at room temperature after several weeks. They were mechanically separated and washed with cold water. **Complex 3.** Anal. calcd for $FeC_{40}H_{26}N_{20}O_2$ (mixture of **3-A** and **3-B**): C, 55.9; N, 31.0; H, 3.3%. Found: C, 56.0; N, 30.8; H, 3.2%. IR data (ν, cm^{-1}) for **3** (similar IR spectra for **3-A** and **3-B**): 3441(br), 3260(m), 3236(m), 2237(s), 2210(s), 2199(s), 1653(w), 1636(m), 1615(w), 1590(m), 1495(s), 1429(m), 1379(m), 1346(m), 1173(m), 1060(m), 999(m), 788(m), 693(m).

Physical Techniques. Infrared spectra were recorded in the range 4000−200 cm^{-1} as KBr pellets on a FT-IR NEXUS NICOLET Spectrometer. ^{13}C NMR spectra were recorded on a Bruker AMX 3-400 spectrometer. Chemical shifts are reported in δ units (parts per million) downfield from the solvent resonance as an external reference. Variable-temperature susceptibility measurements were carried out in the temperature range 2−400 K with applied magnetic fields of 0.1 T on polycrystalline samples with a Quantum Design MPMS-XL-5 SQUID magnetometer. The susceptibility data were corrected for the sample holders previously measured using the same conditions and for the diamagnetic contributions of the salt as deduced by using Pascal's constant tables ($\chi_{dia} = -451.8 \times 10^{-6}$, -561×10^{-6}, and -583.8×10^{-6} emu·mol^{-1} for **1**−**3**, respectively). Elemental analyses were obtained from the Service Central d'Analyses (Vernaison).

Crystallographic Data Collections and Structural Determinations. Crystallographic studies of complex **1** were performed at 293 K using an Oxford Diffraction Xcalibur κ-CCD diffractometer and at 400 K using a Brucker-Nonius κ-CCD diffractometer, both with Mo Kα radiation. A small crystal was used to collect the data. At 293 K, the full sphere data collection was performed using 0.5° φ scans and ω scans with an exposure time of 50 s per frame. The unit cell determination and data reduction were performed using the CrysAlis program suite[29] on the full set of data. At 400 K, a single-crystal oven was used to heat the sample (Enraf-Nonius crystal heater FR 559). The obstruction generated by the oven constrained us to fix the κ circle first at 0° and then at −25°. The data collection was then performed using 1° φ scans on 360° at $\kappa = 0$ and two 1° ω scans on 125° at $\kappa = -25°$ and two fixed φ position separated by 90°. For every set of data, an exposure time of 60 s per frame was used. The unit cell determination and data reduction were performed using the denzo and scalepack program[30] on the full set of data. Crystallographic studies of complexes **2**, **3-A**, and **3-B** were performed at 100 and 293 K using an Oxford Diffraction Xcalibur κ-CCD diffractometer with Mo Kα radiation. The full sphere data collection was performed using 0.75° φ scans and ω scans with an exposure time of 45 s per frame. The unit cell determination and data reduction were performed using the CrysAlis program suite[29] on the full set of data. For the four complexes, the crystal structures were solved by direct methods and successive Fourier difference syntheses with the Sir97 program[31] and refined on F^2 by weighted anisotropic full-matrix least-squares methods using the SHELXL97 program.[32] Both pieces of software were used within the WINGX package.[33] No absorption correction was needed owing to the low absorption coefficient of these complexes.

Results and Discussion

Synthesis and General Characterization. To a water/methanol solution containing $FeCl_2 \cdot 4H_2O$ and abpt in a 1:2 ratio was added a solution of the corresponding polynitrile potassium salt. Each complex (**1**, **2**, **3-A**, and **3-B**) has been obtained as prismatic-pellet single crystals after slow evaporation of the corresponding solution. As described in the experimental section, in the case of complex **3**, two different polymorphs (**3-A** and **3-B**), exhibiting two different molecular arrangements, have been obtained. Furthermore, it was difficult to simply identify each polymorph on the basis of the shape and color of the single crystals since both polymorphs have been obtained as red prismatic single crystals. However, it is worthy to note that both polymorphs are not concomitant and grow in separate sets. Powder diffraction appears as the best way to identify each polymorph, but it was not easy to achieve due to the low yields obtained in the silicate gel procedure. Thus, each polymorph was unambiguously identified using single-crystal X-ray diffraction on several samples. Nevertheless, it was not possible to determine which parameter governs the formation of one polymorph rather than the other. In order to obtain a specific experimental procedure for each polymorph, we have performed several syntheses of **3** using diffusion, through the silicate gel method. Single X-ray diffraction showed that polymorph **3-B** is the unique product formed in all syntheses performed in such a way. The IR spectra of compounds **1**−**3** show similar patterns to those of their corresponding potassium salts (K(tcm) for **1**, K(tcnome) for **2**, and K(tcnoet) for **3**). In each case, three intense absorption bands (2171, 2188, and 2241 cm^{-1} for **1**; 2192, 2201, and 2218 cm^{-1} for **2**; 2199, 2210, and 2237 cm^{-1} for **3**) are assigned to the ν_{CN} stretching vibrations. For complexes **1** and **3**, the two first absorption bands are in the range of those observed in the corresponding spectra of the potassium salts containing the weakly coordinated polynitrile anions (K(tcm): 2128, 2177, cm^{-1}; K(tcnoet): 2149, 2166, 2204 cm^{-1}), while the third absorption bands (2241 cm^{-1} for **1** and 2237 cm^{-1} for **3**) are significantly shifted to higher wavenumbers. This is in good agreement with the presence of both coordinated and uncoordinated CN groups in both iron complexes, as shown by the X-ray structures. On the other hand, the three intense absorption bands in the spectrum of complex **2** are not very different from those pointed on the IR spectrum of K(tcnome) (2176 and 2208 cm^{-1}); this observation can be explained by the possible presence of coordinated CN groups in the potassium salt. To confirm this assumption, we have performed the synthesis of the tetraethylammonium salt containing the uncoordinated $(tcnome)^-$; the IR spectrum exhibits two strong absorption bands (2180, 2194 cm^{-1}) assigned to the ν_{CN} stretching vibrations. A comparison of these absorption bands to those of the IR spectrum of

(29) *CrysAlis Software system*, version 1.171; *Xcalibur CCD system*; Oxford Diffraction Ltd.: Oxfordshire, U.K., 2005.
(30) *COLLECT*, Nonius: Delft, The Netherlands, 1998.
(31) Altomare, A.; Burla, M. C.; Camalli, M.; Cascarano, C.; Giacovazzo, C.; Guagliardi, A.; Moliterni, A. G. G.; Polidori, G.; Spagna, R. *J. Appl. Crystallogr.* **1999**, *32*, 115.
(32) Sheldrick, G. M. *SHELX97*; University of Göttingen: Göttingen, Germany, 1997.
(33) Farrugia, L. J. *J. Appl. Crystallogr.* **1999**, *32*, 837.

Table 1. Summary of X-Ray Data Collection and Refinement for [Fe(abpt)$_2$(tcm)$_2$] (**1**), [Fe(abpt)$_2$(tcnome)$_2$] (**2**), and [Fe(abpt)$_2$(tcnoet)$_2$] (**3-A** and **3-B**)

	1		**2**		**3-A**		**3-B**	
formula[a]	$C_{32}H_{20}Fe_1N_{18}$		$C_{40}H_{26}Fe_1N_{20}O_2$		$C_{42}H_{30}Fe_1N_{20}O_2$		$C_{42}H_{30}Fe_1N_{20}O_2$	
fw	712.51		874.66		902.71		902.71	
cryst syst	monoclinic		monoclinic		triclinic		triclinic	
space group	*P*2/c		*P*2$_1$/*n*		*P*$\bar{1}$		*P*$\bar{1}$	
T (K)	293K	400K	293 K	100 K	293K	100K	293K	100K
a (Å)	9.027(1)	9.294(1)	10.832(1)	10.721(1)	8.806(1)	8.714(1)	8.922(1)	8.865(1)
b (Å)	10.712(1)	10.851(1)	14.912(2)	14.823(1)	10.526(1)	10.432(1)	10.455(1)	10.411(1)
c (Å)	16.485(2)	16.750(1)	12.052(1)	11.962(1)	12.043(1)	11.907(2)	22.253(2)	22.007(2)
α (deg)	90	90	90	90	69.30(1)	69.15(1)	93.15(1)	93.55(1)
β (deg)	92.34(1)	91.10(1)	90.62(1)	90.10(1)	85.28(1)	84.09(1)	92.81(1)	93.97(1)
γ (deg)	90	90	90	90	85.76(1)	86.84(1)	94.16(1)	94.52(1)
V (Å^3)	1593(1)	1689(1)	1946(1)	1901(1)	1039(1)	1006(1)	2064(1)	2015(1)
Z[a]	2	2	2	2	1	1	2	2
color	red	yellow	yellow	yellow	red	red	red	red
μ(mm^{-1})	0.53	0.5	0.454	0.465	0.428	0.442	0.431	0.441
R_{int}	0.036	0.044	0.078	0.047	0.034	0.026	0.063	0.057
R1[b]	0.0432	0.046	0.056	0.043	0.035	0.037	0.067	0.058
wR2[c]	0.098	0.095	0.040	0.045	0.065	0.085	0.112	0.108
GOF[d]	1.079	1.054	0.981	1.041	0.906	1.041	1.097	1.074

[a] For complexes **1**, **2** and **3-A**, the asymmetric unit contains 0.5 of the chemical formula. For **3-B**, the asymmetric units contains two halves of the chemical formula located on two different inversion centers. [b] $R1 = |F_o - F_c|/F_o$. [c] $wR2 = \{\sum[w(F_o^2 - F_c^2)^2]/\sum[w(F_o^2)^2]\}^{1/2}$. [d] $GOF = \{\sum[w(F_o^2 - F_c^2)^2]/(N_{obs} - N_{var})\}^{1/2}$.

complex **2** (2192, 2201, and 2218 cm^{-1}) allows us to confirm the presence of both coordinated and uncoordinated CN groups in complex **2**. However, the third band observed for **2** appears significantly less shifted to high energy than those of the two polymorphs of compound **3**, suggesting a different coordination mode for **3**.

Crystal Structure Descriptions. [Fe(abpt)$_2$(tcm)$_2$] (**1**) and [Fe(abpt)$_2$(tcnome)$_2$] (**2**) crystallize in the monoclinic *P*2/*c* and *P*2$_1$/*n* space groups, respectively, whereas the two polymorphs of [Fe(abpt)$_2$(tcnoet)$_2$] (**3-A** and **3-B**) crystallize in the triclinic space group *P*$\bar{1}$. For all complexes, there is not any structural transition within the studied temperature range (100−400 K). The unit cell parameters and crystal and refinement data are summarized in Table 1. The following general structural descriptions are given at 293 K. The pertinent structural modifications induced by cooling or warming will be discussed further in the paragraph dealing with structural and magnetic property relationships. Figures 1−3 show perspective ORTEP[34] drawings of complexes **1**−**3**, respectively. In each case, except for complex **3-B**, the asymmetric unit consists of an iron atom on an inversion center, one abpt molecule, and one polynitrile anion coordinated to the metal (Figures 1, 2, and 3a). The asymmetric unit of the polymorph **3-B** only differs by the presence of two crystallographically independent iron centers instead of one, where both metal ions are located on two inversion centers (Figure 3b). The two independent molecules generated around these two centers will be noted **B1** and **B2** in the following discussion.

The molecular structure of all of the complexes consists of discrete [Fe(abpt)$_2$L$_2$] complexes where two equivalent chelating abpt ligands stand in the equatorial plane and two equivalent terminal polynitrile anions (L) complete the coordination sphere in trans positions (Figures 1−3). Each Fe(II) ion is in a distorted [FeN$_6$] octahedral environment; selected bond lengths and bond angles are summarized in Table 2.

(34) Farrugia, L. J. *J. Appl. Crystallogr.* **1997**, *30*, 565.

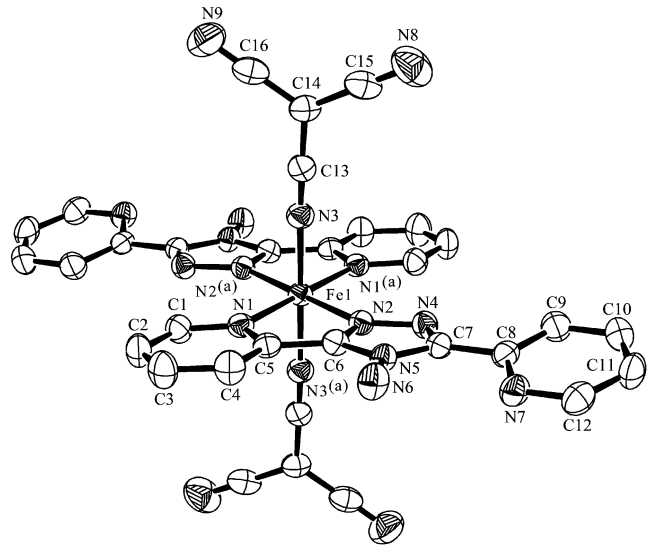

Figure 1. ORTEP drawing (50% probability ellipsoid) of the discrete complex of **1** showing the asymmetric unit, the atom labeling scheme, and the coordination environment of the iron ion. Code of equivalent position: (a) 1 − *x*, −*y*, 1 − *z*.

The geometry and bond lengths and angles of the tcm$^-$ in **1** are in good agreement with those observed in various coordination complexes involving this anion.[35] For (tcnome)$^-$ and (tcnoet)− anions, the presence of the supplementary *π* electron systems of the cyano groups induce strong electronic delocalization, as previously observed in related tcnoet$^-$ coordination compounds:[22] In each complex (**2**, **3-A**, **3-B** (molecule **B1**), and **3-B** (molecule **B2**)), the three central C atoms of both anionic ligands (C17, C18, and C19, Figures 2 and 3) present an sp^2 hybridization, as indicated by the sum of the three angles around them (359.7−360.0° in each

(35) See, for example:(a) Yuste, C.; Bentama, A.; Stiriba, S.-E.; Armentano, D.; DeMunno, G.; Lloret, F.; Julve, M. *Dalton Trans.* **2007**, 5190. (b) Li, B.-L.; Wang, X.-Y.; Zhu, X.; Gao, S.; Zhang, Y. *Polyhedron* **2007**, *26*, 5219. (c) Jones, L. F.; O'Dea, L.; Offermann, P.; Jensen, P.; Moubaraki, B.; Murray, K. S. *Polyhedron* **2006**, *25*, 360. (d) Thétiot, F.; Triki, S.; Sala-Pala, J.; Golhen, S. *Inorg. Chim. Acta* **2005**, *358*, 3277. (e) Batten, S. R.; Murray, K. S. *Coord. Chem. Rev.* **2003**, 103, and references therein.

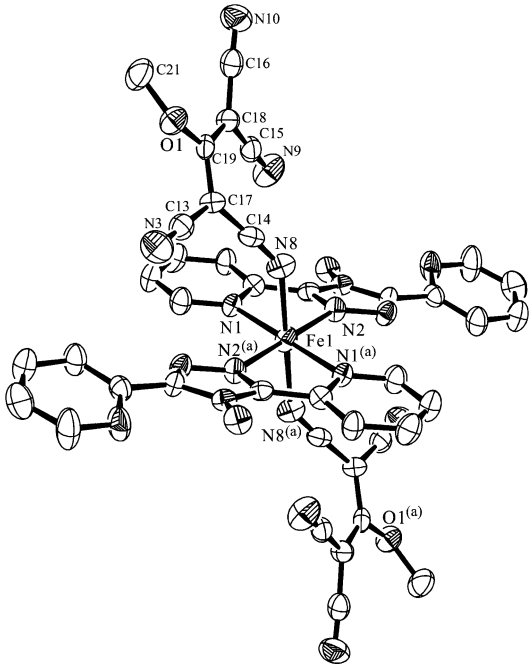

Figure 2. ORTEP drawing (50% probability ellipsoid) of the discrete complex of **2** showing the asymmetric unit, the atom labeling scheme, and the coordination environment of the iron ion. Code of equivalent position: (a) $-x$, $-y$, $-z$.

complex). Two additional facts support the idea of electron delocalization over the three central C atoms: (i) the six central C−C bond distances (1.402−1.421 Å) are longer than a normal C═C double bond (1.34 Å) and close to those of benzene and (ii) the C19−O1 bond distances (1.345−1.375 Å) are much shorter than the normal C−O single bond, suggesting that the two central C−C bonds and the C19−O1 bond present a partial double character. Such a partial double bond character does not avoid fast rotations around the two central C−C bonds, as shown by the ^{13}C NMR spectrum, since a single signal is observed for the four C≡N groups of each free anion (see the Experimental Section). Although both $-C(CN)_2$ units are planar (the maximum deviation from the average plane is 0.025 Å), it is noteworthy that, except in molecule **B2** of polymorph **3-B**, the polynitrile ligands deviate significantly from planarity despite their highly conjugated system. Thus, the two planar $C(CN)_2$ wings are tilted out of the plane containing the central fragment C17−C19(O1)−C18 and form dihedral angles in the range 20.9−30.3°, similar to those observed in the related $(tcnoet)^-$ ligand, where values in the range 30.9−32.7° have been found. In contrast, the $(tcnoet)^-$ ligand of the **B2** molecule in polymorph **3-B** (Figure 3b) is nearly planar. The two planar $C(CN)_2$ wings are tilted out of the plane containing the central fragment C17−C19(O1)−C18 and form a dihedral angle of 3.7°, significantly smaller than the corresponding angles mentioned above for complexes **2** and **3-A** and for molecule **B1** of polymorph **3-B**. This unexpected planarity of the ligand can also be observed in the low value (0.13 Å) of the maximum deviation from the average plane of the organic ligand (without considering the terminal ethyl group). As expected, such deviation from the mean plane is much more important in complexes **2** (0.55 Å) and **3-A** (0.69 Å) and in molecule **B1**in polymorph **3-B** (0.62 Å).

Careful examination of the intermolecular contacts in the four complexes (Figure 4) reveals that the main contacts are attributed to (i) π-stacking interactions between two abpt ligands and two polynitrile anions and (ii) hydrogen-like interactions involving one of the hydrogen atoms of the amine group and a nitrogen atom of one CN group of the anion from a neighboring molecule. The shortest intermolecular contacts are gathered in Tables 3 and 4. These intermolecular interactions lead to two types of crystal packing: a first one where abpt molecules stack parallel (as found in compounds **2** and **3-A**; Figure 4b and c, respectively) and a second type where the abpt molecules stack perpendicular (as found in compounds **1** and **3-B**; Figure 4a and d, respectively). These two types will be denoted here as parallel- and perpendicular-packing, respectively. As expected, the main difference between the two polymorphs of compound **3** lies in these intermolecular arrangements since the packing is parallel in **3-A** and perpendicular in **3-B**, as clearly shown in Figure 4c and d, respectively.

In addition, as already observed for $[Fe(abpt)_2X_2]$ complexes ($X = NCS^-$, $NCSe^-$),[10] examination of the intermolecular contacts through the abpt ligands (Table 4) reveals two kinds of π stacking, which are denoted here as frontal and sideways π stacking. As shown in Figure 5, complexes **1**, **3-A**, and **3-B** adopt the frontal π stacking, whereas complex **2** presents the sideways one. As a consequence, the abpt molecules stack more efficiently in compounds **1**, **3-A**, and **3-B** than in compound **2**. Indeed, according to Table 4, at least five short C···C or C···N close contacts ranging from 3.32 to 3.60 Å are observed in the case of frontal π stacking, while the sideways conformation leads to only two short C···N contacts. Thus, the abpt molecules overlap almost completely for compounds **1**, **3-A**, and **3-B**, whereas the π stacking is less efficient and leads to much weaker $\pi-\pi$ interactions in compound **2**.

Magnetic Properties. Variable-temperature susceptibility measurements were carried out in the temperature range 2−400 K for all compounds. The thermal dependencies of the product of the molar magnetic susceptibility times the temperature ($\chi_m T$) for the four complexes are depicted in Figure 6. For complex **2**, the $\chi_m T$ product shows a room temperature value of 3.25 emu·K·mol^{-1}, which remains constant in the temperature range 40−400 K. This value, slightly bigger than the spin-only value calculated for an isolated metal ion with $S = 2$ (3.0 emu·K·mol^{-1}), indicates that complex **2** is essentially paramagnetic and presents the high-spin ($S = 2$) configuration in the whole temperature range. Below 40 K, the $\chi_m T$ product sharply decreases to reach a value of ca. 2.0 emu·K·mol^{-1} at 2 K. This decrease at low temperatures can be attributed to the presence of a zero field splitting of the $S = 2$ ground spin state.

For complexes **1**, **3-A**, and **3-B**, the magnetic behaviors are different from that described above for complex **2**, since their $\chi_m T$ products are close to zero in the temperature range 2−260 K, indicating that they are in the low spin state ($S = 0$) below room temperature.

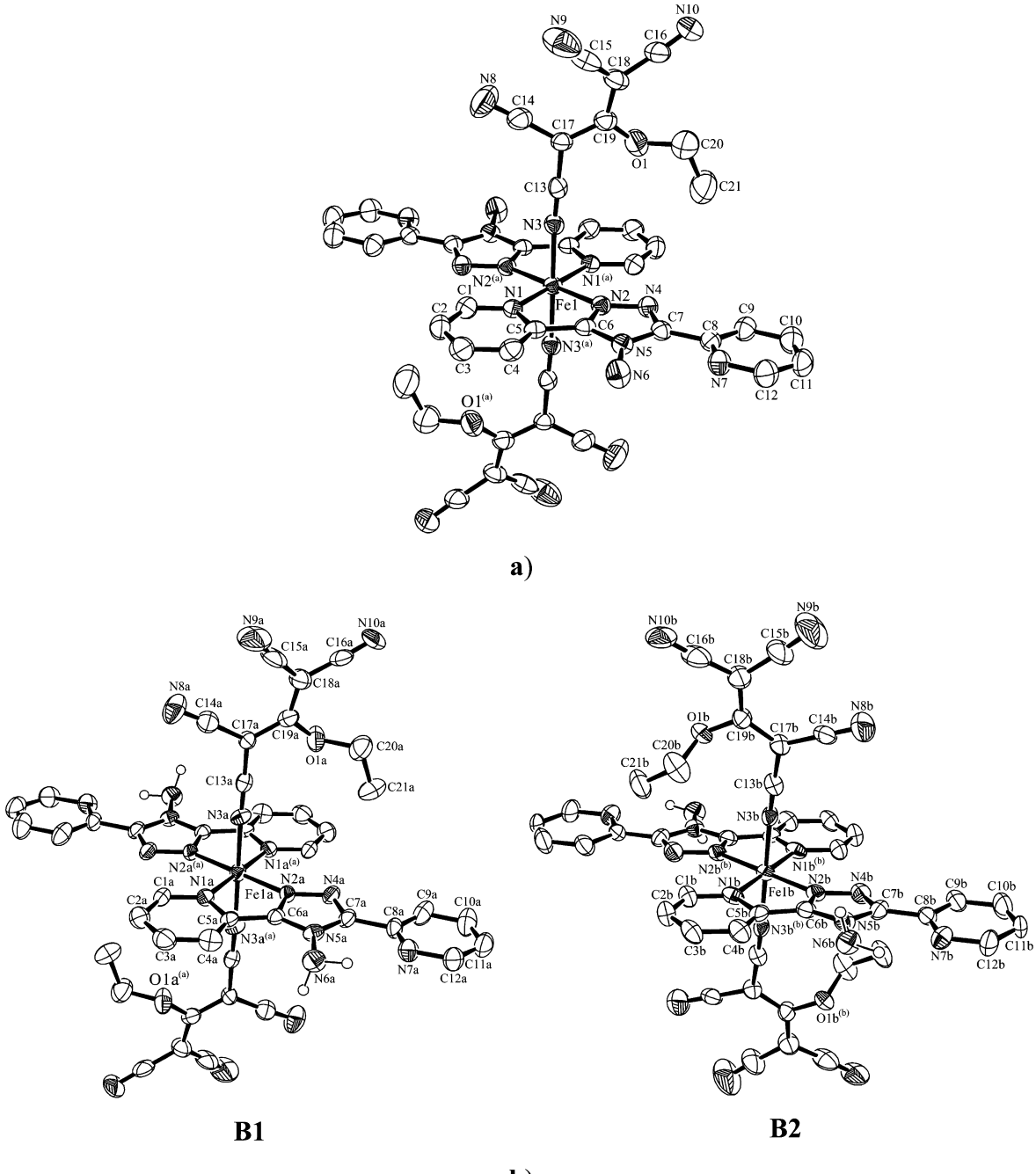

Figure 3. ORTEP drawing (50% probability ellipsoid) of discrete complex of **3** showing the asymmetric unit, the atom labeling scheme, and the coordination environment of the iron ions: (a) polymorph **3-A** and (b) polymorph **3-B**. Codes of equivalent positions: (a) $-x, -y, -z$; (b) $-x, -y, 1-z$.

Table 2. Selected Bond Lengths (Å) and Angles (deg) in Complexes **1**, **2**, **3-A**, and **3-B** at 293 K

			3-B			
	1	**3-A**	**B1**	**B2**		**2**
Fe1−N3	1.941(3)	1.936(2)	1.933(6)	1.933(6)	Fe1−N8	2.167(3)
Fe1−N2	1.996(2)	1.982(2)	1.988(6)	1.961(6)	Fe1−N2	2.125(3)
Fe1−N1	2.022(2)	2.013(2)	1.998(6)	2.019(5)	Fe1−N1	2.185(3)
N1−Fe1−N2	80.2(1)	80.3(1)	80.2(3)	79.6(3)	N1−Fe1−N2	76.8(1)
N3−Fe1−N1	89.5(1)	92.1(1)	91.3(2)	88.2(2)	N8−Fe1−N1	91.2(1)
N3−Fe1−N2	88.5(1)	90.6(1)	91.2(2)	88.6(2)	N8−Fe1−N2	83.4(1)
C13−N3−Fe1	177.6(2)	175.5(2)	177.0(6)	171.0(6)	C14−N8−Fe1	143.5(3)

For **1**, the magnetic properties were measured in both cooling and warming modes, but no thermal hysteresis effects were detected. When warming, $\chi_m T$ remains unchanged until 260 K, where it begins to increase rapidly to reach the beginning of a plateau at 400 K with a value of ca. 3.1 emu·K·mol^{-1}, which is in agreement with the presence of a HS $S = 2$ ground state in **1**. This magnetic behavior is the signature of a spin transition with $T_{1/2} = 336$ K. The

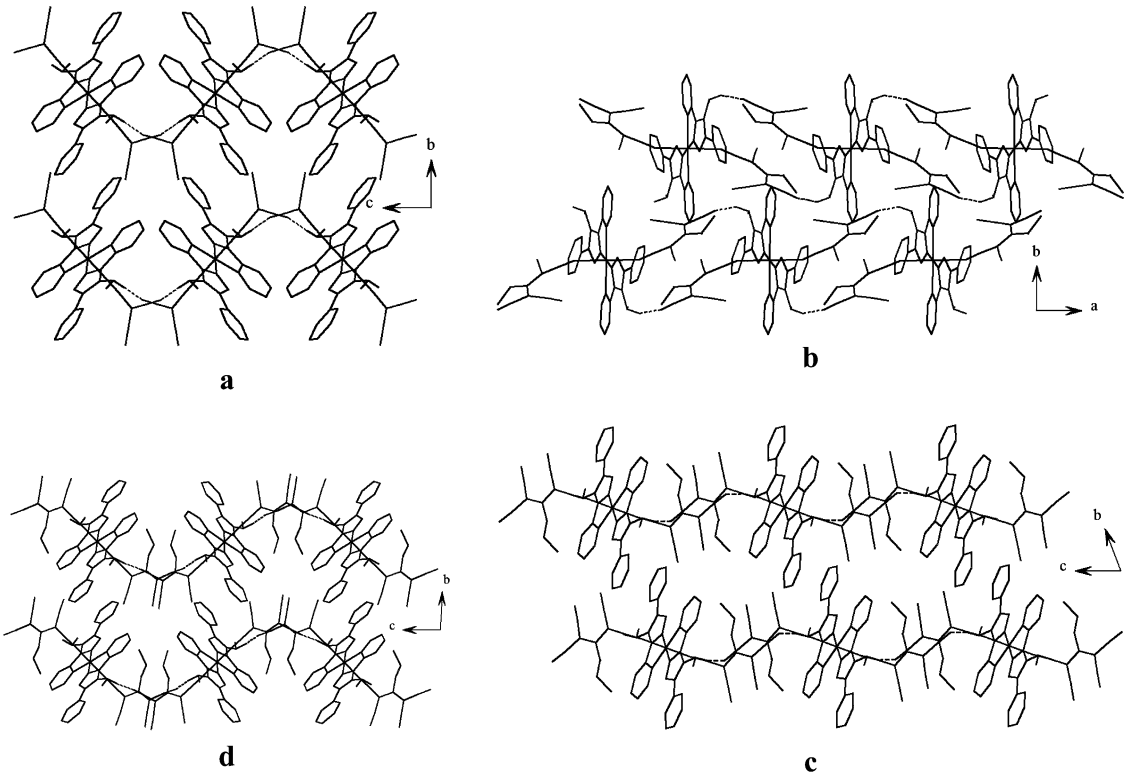

Figure 4. Crystal packing of complexes **1** (a), **2** (b), **3-A** (c), and **3-B** (d).

Table 3. Main Hydrogen-Like Interactions

	D−H···A	D−H (Å)	H···A (Å)	D···A (Å)	D−H···A (deg)
1	N6−H5···N9	0.83(5)	2.35(5)	3.07(1)	146(4)
2	N6−H5···N10	0.91(4)	2.31(4)	3.08(1)	142(3)
3-A	N6−H5···N10	0.94(4)	2.40(3)	3.13(1)	136(2)
3-B (**B1**)	N6A−H5A···N10B	1.00(4)	2.13(5)	3.07(1)	157(3)
3-B (**B2**)	N6B−H5B···N10A	1.00(8)	2.19(8)	3.13(1)	156(6)

Table 4. Main Intermolecular π-Stacking Contacts (Å)

				3-B	
	1	**2**	**3-A**	**B1**	**B2**
C···C	3.32(1)		3.37(1)	3.32(1)	3.38(1)
	3.36(1)		3.39(1)	3.39(1)	3.41(1)
	3.57(1)		3.43(1)	3.46(1)	3.46(1)
	3.57(1)		3.52(1)	3.48(1)	3.60(1)
			3.53(1)	3.53(1)	
			3.59(1)	3.60(1)	
C···N	3.42(1)	3.36(1)			3.34(1)
		3.41(1)			3.38(1)
					3.43(1)

abruptness of such a transition can be estimated by the previously defined parameter denoted ΔT_{80}, corresponding to the temperature gap needed to undergo the spin transition from 80% LS to 80% HS.[36−38] Compound **1** presents a relatively abrupt spin transition with $\Delta T_{80} \sim 38$ K (Figure 6). For compound **3**, the magnetic properties were measured for both polymorphs. As for **1**, the $\chi_m T$ product is close to zero at low temperatures, which indicates a low-spin state for the iron(II) ions. The $\chi_m T$ product remains unchanged until 270 K for polymorph **3-A** and 300 K for polymorph **3-B** (Figure 6) and then increases to reach 1.99 and 1.92 $cm^3 \cdot K \cdot mol^{-1}$, respectively, at 400 K. These significant increases correspond to a spin-state conversion of about 60% of the iron centers from LS to HS in both complexes. This spin transition occurs at $T_{1/2} = 377$ K for polymorph **3-A** and $T_{1/2} = 383$ K for polymorph **3-B**. As the limit temperature of the magnetometer was reached, the completeness of the transition could not be observed. Nevertheless, the abruptness of the transitions can be estimated at $\Delta T_{80} \sim 87$ K for polymorph **3-A** and $\Delta T_{80} \sim 60$ K for polymorph **3-B**. Thus, the spin transition seems to be more cooperative for polymorph **3-B** than for polymorph **3-A**.

Discussion. The four complexes studied herein present similar molecular structures but different magnetic behaviors. In particular, compound **2** does not undergo any spin transition, remaining HS in the whole temperature range, whereas compounds **1**, **3-A**, and **3-B** present a spin transition between 300 and 400 K. The exception of complex **2** may probably be explained by the coordination modes of the complexes. Indeed, in both polymorphs of **3**, the polynitrile anion coordinates the metal ion via the nitrogen N3 of the nitrile group, in the cis position from the ethoxy group.

(36) Kröber, J.; Audière, J.-P.; Claude, R.; Codjovi, E.; Kahn, O.; Haasnoot, J. G.; Grolière, F.; Jay, C.; Bousseksou, A.; Linarès, J.; Varret, F.; Gonthier-vassal, A. *Chem. Mater.* **1994**, *6*, 1404.
(37) Marchivie, M.; Guionneau, P.; Létard, J.-F.; Chasseau, D. *Acta Crystallogr., Sect. B* **2003**, *59*, 479.
(38) Marchivie, M.; Guionneau, P.; Létard, J.-F.; Chasseau, D. *Acta Crystallogr., Sect. B* **2005**, *B61*, 25.

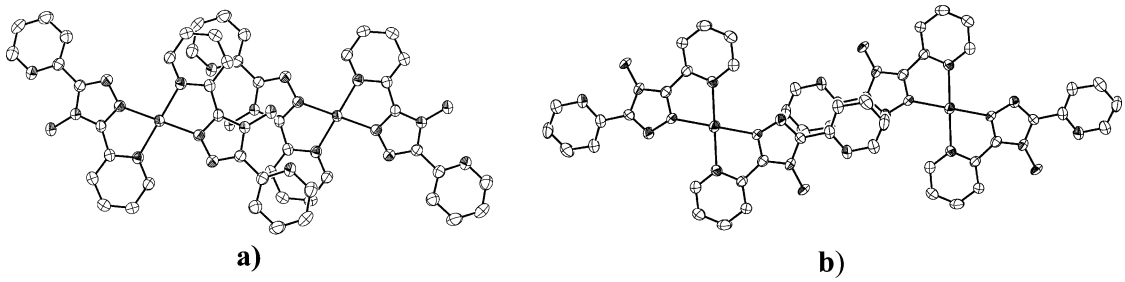

Figure 5. ORTEP perspective views of the abpt π stacking: (a) frontal π stacking in complex **1** (similar π stacking in **3-A** and **3-B** polymorphs) and (b) sideways π stacking in complex **2**.

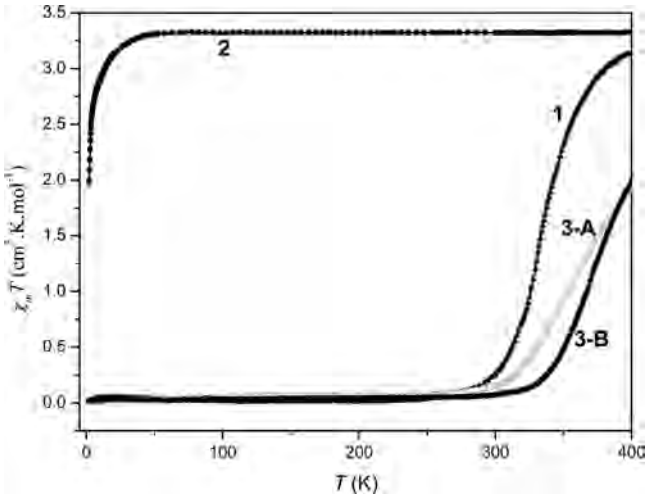

Figure 6. Thermal variation of the $\chi_m T$ product for **1**, **2**, **3-A**, and **3-B**.

Scheme 2. Coordinated CN Groups in **2** (a) and in Both Polymorphs **3-A** and **3-B** (b)

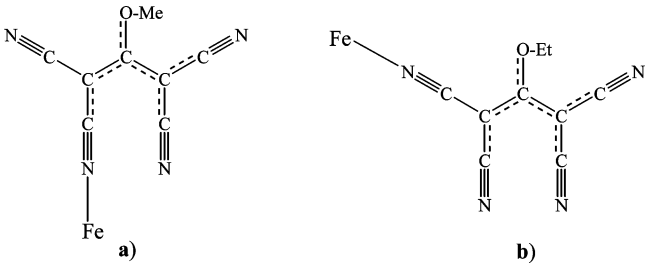

Conversely, in **2**, the polynitrile anion coordinates the metal ion via the nitrogen N8 of the nitrile group, in the trans position from the ethoxy group (Scheme 2). These distinct coordination modes may induce different ligand field energies, which explain the different spin states at room temperature as well as the absence of a spin transition in compound **2**.

The significance of the structural parameters on spin transition complexes is now well-known,[5,39−42] and their implication on the magnetic properties has been clarified more recently by the introduction of the distortion parameters

Table 5. Fe−N Distances and Distortion Parameters for Each Iron Coordination Sphere

	T (K)	Fe−N (Å)	π (deg)	Θ (deg)	HS (%)
1	293	1.986	47(2)	182(3)	∼0 HS
1	400	2.157	69(2)	264(3)	100 HS
2	293	2.159	84(2)	249(4)	100 HS
3-A	293	1.977	50(1)	180(2)	∼0 HS
3-A	100	1.971	50(1)	170(3)	0 HS
3-B (**B1**)	293	1.973	49(4)	182(7)	∼0 HS
3-B (**B2**)	293	1.971	54(4)	192(7)	∼0 HS
3-B (**B1**)	100	1.970	49(3)	184(5)	0 HS
3-B (**B2**)	100	1.965	53(3)	179(5)	0 HS

Σ[43,44] and Θ:[37,38,41] Σ is the sum of the deviation from 90° of the 12 cis angles of the FeN_6 octahedron, and Θ (trigonal distortion parameter) is the sum of the deviation from 60° of the 24 trigonal angles of the projection of the FeN_6 octahedron onto its trigonal heads. Typical values expected for an FeN_6 octahedron in Fe(II) complexes involving bisdentate ligands are Σ ∼ 40−60° and Θ ∼ 130−180° for Fe(II) in the low spin state and Σ ∼ 70−85° and Θ ∼ 220−280° for Fe(II) in the high spin state. It has been noticed that the Θ parameter plays an important role determining spin transition features such as the characteristic temperatures of the phenomenon and the abruptness of the spin transitions. Thus, in compounds **1** and **3** (polymorphs **3-A** and **3-B**), where spin transitions above room temperature are observed (Figure 6), the average Fe−N distances at room temperature (1.97−1.98 Å) and the distortion of the metal coordination sphere (Σ = 47−54°) are characteristic of an Fe(II) ion in the low spin state (Table 5).[41,44,45] Unfortunately, due to crystal decomposition, the crystal structures of both polymorphs could not be obtained above 400 K. However, single-crystal X-ray diffraction data could be collected for compound **1**, which reaches the full high spin state at 400 K. Its crystal structure has been solved at 400 K and leads to sufficiently good-quality data. At this temperature, a strong modification of the iron coordination sphere is observed for this complex. The average Fe−N distances (d_{Fe-N} = 2.157(3) Å) and the distortion of the metal coordination sphere (Σ = 69(2)° and Θ = 264(3)°) increase significantly. This particular behavior is the structural signature of a spin state transition from LS to HS. The values of the average Fe−N

(39) Real, J.-A.; Gallois, B.; Granier, T.; Suez-Panama, F.; Zarembowitch, J. *Inorg. Chem.* **1992**, *31*, 4972.
(40) Real, J.-A.; Gaspar, A. B.; Niel, V.; Muñoz, M. C. *Coord. Chem. Rev.* **2003**, *236*, 121.
(41) Guionneau, P.; Marchivie, M.; Bravic, G.; Létard, J.-F.; Chasseau, D. *Top. Curr. Chem.* **2004**, *234*, 97.
(42) König, E. *Prog. Inorg. Chem.* **1987**, *35*, 527.
(43) Deeney, F. A.; Harding, C. J.; Morgan, G. G.; McKee, V.; Nelson, J.; Teat, S. J.; Clegg, W. *Dalton Trans.* **1998**, 1837.
(44) Guionneau, P.; Marchivie, M.; Bravic, G.; Létard, J.-F.; Chasseau, D. *J. Mater. Chem.* **2002**, *12*, 2546.
(45) Guionneau, P.; Brigouleix, C.; Barrans, Y.; Goeta, A. E.; Létard, J.-F.; Howard, J. A. K.; Gaultier, J.; Chasseau, D. *C.R. Acad. Sci., Ser. IIc: Chim.* **2001**, *4*, 161.

Scheme 3. π Stacking of the abpt Ligands in Complexes **1**, **2**, **3-A**, and **3-B**: (a) Frontal π Stacking and (b) Sideways π Stacking

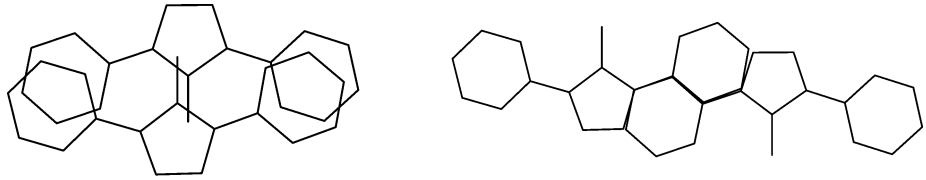

a) b)

Table 6. abpt π Stacking and Magnetic Properties in the Series $[Fe(abpt)_2(A)_2]$ (A = Terminal Monoanion N Ligand)

	π stacking	spin transition	$T_{1/2}$ (K)	ΔT_{80} (K)	reference
1	frontal	gradual	336	38	this work
2	sideways	none (HS)			this work
3-A	frontal	gradual	378	87	this work
3-B	frontal	gradual	383	60	this work
$[Fe(abpt)_2(NCS)_2]$ (A1)	frontal	gradual	180	~40	8, 46
$[Fe(abpt)_2(NCSe)_2]$ (A2)	frontal	gradual	224	~50	8, 46
$[Fe(abpt)_2(dca)_2]$ (A3)	frontal	incomplete	86		7
$[Fe(abpt)_2(tcnq)_2]$ (A4)	frontal	gradual	280	~30	14, 47
$[Fe(abpt)_2(NCS)_2]$ (B1)	sideways	none (HS)			10
$[Fe(abpt)_2(NCSe)_2]$ (B2)	sideways	none (HS)			10

distances as well as the distortion of the metal coordination sphere are in the range expected when 100% of the iron(II) centers are in the high spin state.[41] This observation perfectly fits with the magnetic properties of this complex (Figure 6). Interestingly, compounds **1**, **3-A**, and **3-B** present distinct magnetic behaviors which are driven by the nature of the polynitrile anion ($(tcm)^-$ in **1** and $(tcnoet)^-$ in **3-A** and **3-B**), and by slight differences of the crystal packing in the cases of **3-A** and **3-B**. Thus, compound **1** undergoes a relatively abrupt ($\Delta T_{80} \sim 38$ K) spin transition at $T_{1/2} = 336$ K, whereas compounds **3-A** and **3-B** show less abrupt transitions ($\Delta T_{80} \sim 87$ K and $\Delta T_{80} \sim 60$ K, respectively) at higher temperatures ($T_{1/2} = 377$ K and $T_{1/2} = 386$ K, respectively). It is worth noting that both polymorphs of compound **3** show a different abruptness in their spin transition, and as expected, they also show differences in their coordination sphere. As can be seen in Table 5, when both complexes are in the pure LS state at 100 K, compound **3-B** presents a trigonal distortion ($\Theta = 184(5)$ and $179(5)^\circ$ for **B1** and **B2**, respectively) higher than that of compound **3-A** ($\Theta = 170(3)^\circ$), in agreement with a more abrupt spin transition ($\Delta T_{80} \sim 60$ K) observed for polymorph **3-B** compared to polymorph **3-A** ($\Delta T_{80} \sim 87$ K). This fact confirms the assumption that a more important trigonal distortion induces a more cooperative spin transition. Nevertheless, it would be interesting to complete this observation by obtaining high spin state Θ values in both polymorphs, since they appear to be more significant.[38]

Another structural feature that may play an important role in the magnetic interactions in these iron(II) complexes concerns essentially the intermolecular π stacking observed in all complexes.

As discussed above in the crystal structure descriptions, complexes **1**, **3-A**, and **3-B** present frontal π stacking with several C···C and C···N close contacts between adjacent abpt ligands, while complex **2** adopts a sideways π stacking involving only two C···N close contacts (Scheme 3). This leads to much weaker $\pi-\pi$ interactions in complex **2**. Such structural exception of complex **2** has been evidenced also in magnetic studies, since complexes **1**, **3-A**, and **3-B** present spin transitions between 300 and 400 K, while complex **2** does not undergo any spin transition (HS in the range 2−400 K). According to the different coordination modes already discussed above, it is clear that such exception does not justify any plausible correlation between such π stacking and magnetic properties. However, previous studies already suspected that the sideways conformation, which leads to weaker intermolecular interactions between the complexes, prevents the occurrence of the spin transition in complexes of the related family $[Fe(abpt)_2(NCX)_2]$ (X = S, Se).[8,10,46] Careful examination of the intermolecular π stacking and magnetic properties observed in all related Fe−abpt systems including complexes **1**, **2**, **3-A**, and **3-B** (see Table 6) confirms clearly the assumption that complexes displaying efficient frontal π stacking present spin transition, whereas those involving the less efficient sideways π stacking remain in the HS state in the whole temperature range. It is worth noting that complex **2** presents a similar behavior to the polymorph **B** of $[Fe(abpt)_2(NCS)_2]$ (Table 6);[10] it is then foreseeable that a spin transition may be expected under pressure for this complex.

Conclusions

In summary, we have reported here the syntheses, structural characterization, and magnetic properties of the first spin-crossover complexes containing polynitrile anions. All exhibit discrete similar structures with the general formula $[Fe(abpt)_2(A)_2]$ [A = $(tcm)^-$ (**1**), $(tcnome)^-$ (**2**), $(tcnoet)^-$ (**3-A** and **3-B**)]. Despite their structural similarities, the four complexes display different magnetic behaviors since **2** does not undergo any spin transition, while complex **1** and the two polymorphs of compound **3** (**3-A** and **3-B**) present a

(46) Moliner, N.; Muñoz, M. C.; Koningsbruggen, P. J. v.; Real, J.-A. *Inorg. Chim. Acta* **1998**, *274*, 1.
(47) Cornelissen, J. P.; Van Diemen, J. H.; Groeneveld, L. R.; Haasnoot, J. G.; Spek, A. L.; Reedijk, J. *Inorg. Chem.* **1992**, *31*, 198.

spin transition between 300 and 400 K. The crystal structures of **3-A** and **3-B** could not be obtained above 400 K because the crystals decomposed; however, structural data at 293 and 100 K showed clearly that the differences between the two polymorphs are mostly due to intermolecular arrangements rather than to any change in the local geometry of the complexes since the crystal packing is parallel in **3-A** and perpendicular in **3-B.** In contrast, high-temperature structural data (400 K) of good quality were collected for complex **1.** As expected from the magnetic data, a strong modification of the iron coordination sphere was observed as the structural signature of the spin state transition from LS to HS for this complex. On the basis of the intermolecular π stacking observed for the series described in this paper and for the related complexes involving a similar discrete structure with abpt coligands and an axial anionic terminal ligand, we have shown that complexes displaying frontal π stacking present a spin transition and those involving a sideways π stacking remain in the HS state. The efficiency of the π stacking interactions appears to be, in that way, a key parameter concerning the occurrence of a spin transition. In addition and taking into account the large number of various polynitrile anions that can be synthesized, this first report opens very promising perspectives in the spin crossover field. As shown in this study, for example, a slight chemical modification of these anions ((tcnome)$^-$ and (tcnoet)$^-$) can affect the ligand field energy or the crystal packing and induce drastic modifications of the magnetic properties. It is thus foreseeable that various original magnetic behaviors and a large range of transition temperatures ($T_{1/2}$), even above room temperature, can be obtained. Furthermore, another important feature of these anions concerns their negative charge; we showed in a previous work that the geometry of such anions precludes the possibility of a chelate coordination mode, and therefore, such anions can only act as terminal or bridging ligands through their nitrile groups.[16−27] Thus, to prevent the terminal coordination modes observed in the present work, the use of polynitrile anions involving two negative charges such as (tcno)$^{2-}$ and (tcpd)$^{2-}$ (Scheme 1)[16−26] with appropriate chelating coligands should lead to new spin-crossover systems displaying original extended arrangements and interesting magnetic behaviors, increasing, once more, the potentialities of the family of polynitrile anions.

Acknowledgment. The authors acknowledge the CNRS (Centre National de la Recherche Scientifique), and the European Union for financial support (MAGMANet network of excellence and COST Action D35-WG-0011-05), and the Spanish Ministerio de Educación y Ciencia (Projects MAT2004-03849 and CSD 2007-00010 Consolider-Ingenio in Molecular Nanoscience). G.D. thanks the Ministère de l'Education Nationale, de la Recherche et de la Technologie for a Ph.D. grant.

Supporting Information Available: A CIF file containing data for the compounds mentioned in this work. This material is available free of charge via the Internet at http://pubs.acs.org. CCDC 685469−685476 contain the supplementary crystallographic data for complexes **1**, **3**, **3-A** and **3-B** (**1** at 293 and 400 K, **2** at 293 and 100 K, **3-A** at 293 and 100 K and **3-B** at 293 and 100 K respectively). These data can be obtained free of charge from the Cambridge Crystallographic Data Centre via www.ccdc.cam.ac.uk/data_request/cif.

IC800955R